ACS APPLIED MATERIALS & INTERFACES

Research Article

www.acsami.org

Aptamer-Functionalized Hybrid Carbon Nanofiber FET-Type Electrode for a Highly Sensitive and Selective Platelet-Derived Growth Factor Biosensor

Jaemoon Jun, Jun Seop Lee, Dong Hoon Shin, and Jyongsik Jang*

School of Chemical and Biological Engineering, College of Engineering, Seoul National University (SNU), 599 Gwanangno, Gwanak-gu, Seoul, 151-742 Korea

Supporting Information

ABSTRACT: Precise selectivity and rapid responses to target biomolecules are important in the development of biosensors. In particular, highly sensitive and selective biosensors have been used in clinical treatment to detect factors such as cancer oncoproteins and endocrine disruptors. Herein, highly sensitive liquid electrolyte field-effect transistor (FET) system biosensors were fabricated to detect platelet-derived growth factor (PDGF) using a PDGF-B binding aptamer conjugated with carboxylic polypyrrole-coated metal oxide-decorated carbon nanofibers (CPMCNFs) as the signal transducer. First, CPMCNFs were fabricated using vapor deposition polymerization (VDP) of the carboxylic pryrrole monomer (CPy) on metal oxide-decorated carbon nanofiber (MCNF) surfaces with no treatment for carbon surface functionalization. Furthermore, a 3 nm thick uniformly coated carboxylic polypyrrole (CPPy) layer was formed without aggregation. The CPMCNFs were integrated with the PDGF-B binding aptamer and immobilized on the interdigitated array substrate by covalent anchoring to produce a FET-type biosensor transducer. The PDGF-B binding aptamer conjugated CPMCNF (CPB-Apt) FET sensor was highly sensitive (5 fM) and extremely selective for isoforms of PDGFs. Additionally, the CPB-Apt FET sensor could be reused over a few weeks.

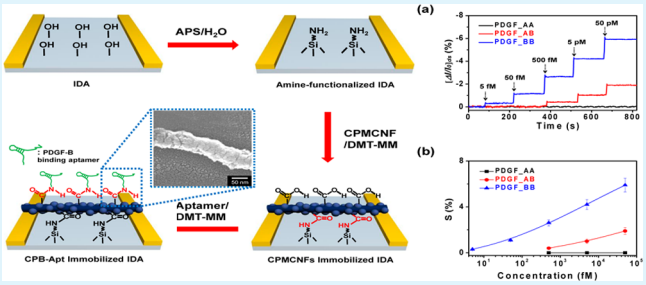

KEYWORDS: *carbon nanofibers, platelet-derived growth factor, electrospinning, biosensor, vapor deposition polymerization*

INTRODUCTION

Recently, studies on the discovery of biomarkers of cancers and the detection of oncogenic proteins that are responsible for the development and progression of cancer have increased because of their essential role in clinical therapy.[1−5] Thus, it is important to develop portable platforms for the sensitive detection of biomarkers, oncogenic proteins, and their molecular variants. Among various approaches, aptamer-based sensors are emerging as an alternative method owing to their highly sensing ability. Aptamers are single-stranded DNA or RNA molecules selected from random pools that are capable of binding with biological entities such as proteins, cells, and small-molecule drugs, peptides, and hormones with high affinity and specificity.[6−9] Furthermore, aptamers may be ideal alternatives to traditional antibodies for use in analytical devices because of their ease of synthesis, high binding affinity, long storage times, and excellent selectivity.[10] Thus, there are many studies on the applicability of aptamers to target disease states such as cancers. These developments have opened new avenues for aptamers to potentially replace more established components in therapeutics and diagnostics.

Platelet-derived growth factor (PDGF) is a protein that regulates cell growth and division. Moreover, over concentration of PDGF is associated with several human disorders such as pulmonary hypertension, atherosclerosis, balloon injury-induced restenosis, organ fibrosis, and tumorigenesis.[11−16] Particluarly, concentration of PDGFs dramatically increased in diseased vessels compared to normal vessels. PDGFs are composed of two different types of monomers, A and B chains (PDGF-AA, PDGF-AB, and PDGF-BB). Among them, PDGF-BB, which is an oncogene protein, is often overexpressed in human malignant tumors and is known as a potential protein marker for cancer diagnosis.[16,17] To detect PFGF-BB, there have been conducted several approaches using fluorescence and electrochemistry methods.[18−24] In fluorescence-based PDGF detection techniques, fluorophore-labeled aptamers have been used to signal binding by monitoring changes in fluorescence intensity through energy transfer. However, the precise target-binding sites and conformational changes in the aptamers are generally unknown. Additionally, conjugation of a fluorophore to an aptamer may weaken the affinity of the aptamer for its ligand. For electrochemistry-based detection using redox reactions, the electrodes are limited to conductive materials, with different linkers used to attach the

Received: May 26, 2014
Accepted: July 14, 2014
Published: July 14, 2014

aptamer to the electrode surface (typically gold), and there is rapid degradation over time.

Traditionally, carbon has been a popular material for biological and electrochemical sensing due to its low cost, high resistance to bio-fouling, bio-compatibility, and high electrical conductivity.[25−28] In various investigations, carbon nanofibers (CNFs) have been shown to be suitable for use as an electron conductor to construct biosensors and as an electrode material to promote electron-transfer reactions of proteins.[29−31] In particular, metal oxide-decorated ultrafine carbon nanofibers (MCNFs) have recently attracted considerable attention because of their remarkable characteristics.[32,33] Specifically, they have excellent electron conductivity and a very high surface-to-volume ratio due to their ultrafine diameter. Additionally, metal oxides on the surface can act as functional sites on the carbon surface; thus, additional functionalization steps are not needed on the carbon surfaces.

Herein, we report a field-effect transistor (FET)-type biosensor to detect the target molecule (PDGF-BB) based on carboxylated polypyrrole-coated MCNFs (CPMCNFs) conjugated with a PDGF-B bindng aptamer (CPB-Abt). To our knowledge, this is the first report of an experimental demonstration of a FET-type biosensor using CPMCNFs as a signal transducer. Binding CPMCNFs onto the FET substrate and immobilizing the PDGF-B binding aptamer provided strong affinity between the aptamer and PDGF-B in a FET-platform suitable for electronic control. Field-induced sensitivities to various PDGF concentrations were observed, eventually leading to the recognition of PDGF-BB at an unprecedentedly low concentration (5 fM). Moreover, this FET platform is also selective for the target analyte and reusable over a large concentration range of the target molecule.

RESULTS AND DISCUSSION

Fabrication of CPMCNFs. Figure 1 illustrates the overall procedure for the fabrication of carboxylated polypyrrole-coated, metal oxide-decorated ultrafine carbon nanofibers (CPMCNFs) via single-nozzle coelectrospinning and vapor deposition polymerization (VDP) methods. First, polyvinylpyrrolidone (PVP) solution containing the ZnO precursor ($ZnAc_2$) was mixed with poly(acrylonitrile) (PAN) solution to make phase-separated polymers in the mixture solution. The mixed polymer solutions were then coelectrospun through a single nozzle. The result was that the phase-separated polymers in the mixed solutions formed core (PAN)/shell (PVP) nanofibers (NFs).[32] The electrospun core/shell NFs were subsequently calcined and carbonized to fabricate ZnO nanonodule-decorated hybrid CNFs (MCNFs). These as-prepared MCNFs were ca. 40 nm in diameter with ca. 10 nm diameter ZnO nanonodules on the surface and were aggregate free (Supporting Information, Figure S1). The MCNFs were then dipped into ethanolic solution containing $FeCl_3$ as an initiator for the VDP step. In the dipping process, ferric cations (Fe^{3+}) were adsorbed on the ZnO nanonodules because of a charge−charge interaction between Fe^{3+} ions and the partial negative charge of oxygen in the ZnO structure (red inset of Figure 1).[34,35] The Fe^{3+}-adsorbed MCNFs were exposed to 3-carboxylated pyrrole (CPy) monomer vapor in a 60 °C vacuum oven for 10 min. Polymerization of CPy monomers occurred via a chemical oxidation polymerization reaction with the Fe^{3+} ions as oxidants on the ZnO surface.[35] As a result, the 3-carboxylated polypyrrole-coated MCNFs (CPMCNFs) formed a 3 nm thick coating layer on the surface (Figure 2). Additionally, there was no aggregation of the CPMCNFs despite the VDP steps, indicating that the Fe cations were uniformly dispersed on the MCNF surfaces.

To confirm the 3-carboxylated polypyrrole (CPPy) layer on the MCNFs, Fourier-transform infrared (FT-IR) spectroscopy was carried out for each CNF, as shown in Figure 3. The spectra of the MCNFs showed the C—C—C symmetric stretching peak at around 850 cm^{-1}.[36] Due to the absence of the CPPy layer, the FT-IR spectrum of MCNFs did not show peaks of functional groups, such as carbonyl and hydroxyl groups. However, the spectra of the CPMCNFs did show peaks at 1554 and 1473 cm^{-1}, corresponding to the C—C and C—N stretching vibrations in the pyrrole ring. Additionally, the peaks at 1294 and 1195 cm^{-1} were attributed to =C—H in-plane vibrations. Furthermore, a peak at 1715 cm^{-1} was observed due to the stretching vibration of C═O and in the carboxylic acid functional group.[36−38] These spectral modulations indicate that the CPPy was coated successfully on the MCNFs through the VDP step.

Fabrication of the CPB-Apt FET Sensor. Figure 4 indicates the procedures for fabricating CPMCNF conjugated with the PDGF-B binding aptamer (CPB-Apt) FET sensor electrode using a condensation reaction of carboxyl and amino groups on the sensor electrode surface. First, CPMCNFs were attached by a chemical reaction, such as a condensation reaction through the carboxyl group (−COOH) of CPPy and the amino group ($-NH_2$) of the (3-aminopropyl)-trimethoxysilane (APS)-treated interdigitated array (IDA) sensor electrode. The condensation reaction of CPPy and the APS-treated electrode formed amide bonding (−CONH−) using condensing agent (4-(4,6-dimethoxy-1,3,5-triazin-2-yl)-4-methylmorpholinium (DMT-MM)).[39−41] Thus, the CPMCNFs covalently anchored on the IDA electrode were fabricated through simple condensation reactions. Then, the amine ($-NH_2$)-modified PDGF-B binding aptamer was immobilized on the CPMCNFs surface through a chemical condensation reaction between the carboxyl group (−COOH) of CPPy and the amino group ($-NH_2$) of the PDGF-B binding aptamer using a condensing agent (DMT-MM). As a result, the

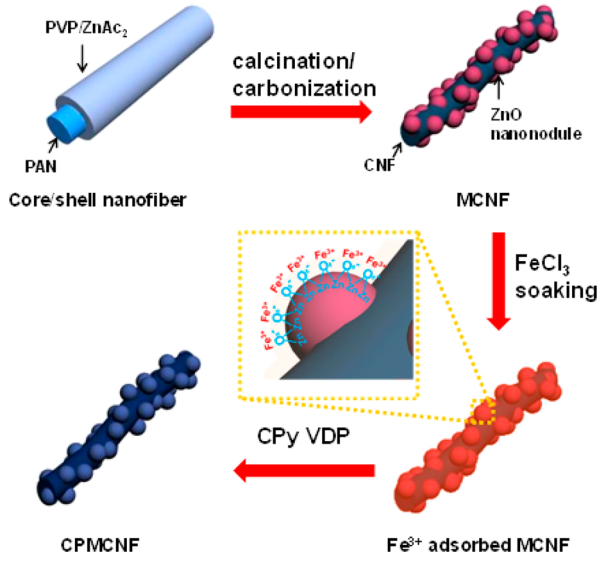

Figure 1. Illustrative diagram of the sequential fabrication steps for 3-carboxylated PPy coated hybrid carbon nanofibers (CPMCNFs).

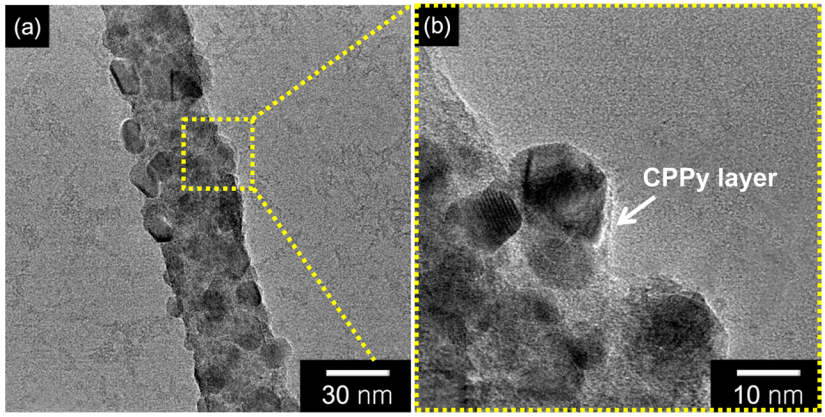

Figure 2. (a) TEM and (b) HR-TEM image of 3-carboxylated PPy coated hybrid CNFs with 3 nm thickness coated layer on the surface.

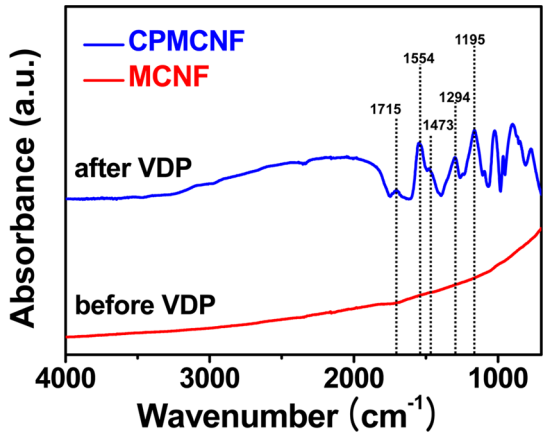

Figure 3. FT-IR spectra of MCNFs (red) and CPMCNFs (blue).

CPB-Apt IDA sensor electrode was fabricated for applying electrolyte-based FET biosensor. The covalent bonding is strong because of the direct chemical bonding. Indeed, this covalent attachment provides some advantages, such as better stability for analyte sensing in the liquid phase and the possibility of control of the functionality of the CPMCNFs, in contrast to a noncovalent approach.

To evaluate the electrical contact of CPB-Apt on the IDA substrate, current−voltage (I−V) characteristics were investigated, as shown in Figure 5a. When the electrical contact is poor, the I−V modulation is nonlinear because of the formation of Schottky barriers at the electrode contact. However, the characteristics of the I−V curve for each CPMCNFs revealed linearity, i.e., ohmic contact, indicating that the CPMCNFs bonded covalently to the IDA surface, providing a good electrical contact. The dI/dV values decreased slightly with the introduction of the PDGF-B binding aptamer on the CPMCNFs surface. Also, increasing the concentration of the PDGF-B binding aptamer on the CPMCNFs decreased the dI/dV values. It can be considered that PDGF-B binding aptamers were nonconductive. Consequently, the difference of the dI/dV values is presumably due to the difference in the resistance. However, the linearity of I−V modulation means that ohmic contact was retained after introduction of the aptamer. Thus, the PDGF-B binding aptamer was effectively incorporated into CPMCNFs with no deterioration in electrical contact or conductivity.

Figure 5b shows a liquid-ion-gated FET-type sensor system based on CPB-Apts. The liquid-ion-gated FET geometry was constructed with the IDA substrate array using CPMCNFs as the conductive channel. The FET sensor platform was surrounded with phosphate-buffered saline (PBS, pH 7.4), which facilitated gate control. The two gold bands of the IDA electrode acted as the source and drain in this FET-type sensor system. Furthermore, the CPB-Apts were immobilized in the liquid electrolyte with no deterioration due to the covalent bonds to the IDA surface. Figure 5c shows the modulation of source-drain current (I_{sd}) and voltage (V_{sd}) under varying gate voltage (V_g) to investigate this FET-type CPB-Apt sensor device. The I_{sd} became more negative when the V_g increased in the negative direction. The subsequent graph indicated that the CPB-Apt FET sensor showed a p-type accumulation mode in the V_g range of 0 to −100 mV. Moreover, the I_{sd} that followed through the CNF network channel was modulated by varying V_g. Negative V_g can give rise to an increase in the oxidation level of the CPMCNF chain. These negative modulations indicate that CPMCNF is a p-type (hole-transporting) transducer in the doped state. These results indicate that the CPB-Apt FET sensor is suitable as an electrochemical biosensor for detecting charged bio-molecules in a PBS buffer solution.

Real-Time Responses of the CPB-Apt FET Sensor. To investigate the performance of the CPB-Apt FET sensor, current changes were measured with various PDGF concentrations in real time at constant V_{sd} (50 mV) and V_g (50 mV). Figure 6a indicates the real-time responses of the CPB-Apt FET sensor to the three types of PDGF (PDGF-AA, PDGF-AB, and PDGF-BB). The CPB-Apt sensor showed a very fast real-time response (<1 s) when the sensor device was exposed to the diverse concentrations of the target PDGF (PDGF-AB and PDGF-BB) solution. Furthermore, the CPB-Apt sensor showed a concentration-dependent decrease in I_{sd} on exposure to PDGF-BB and PDGF-AB. The current decrease is caused by the negative charge of the PDGF-B binding aptamer. The binding aptamer can be screened by the PDGF-B of PDGF-AB/PDGF-BB when the target biomolecule-aptamer complex is formed. The specific binding caused a structural rearrangement of the aptamer, finally leading to a decrease in the negatively charged base state. The decreased negative charge density at the CPB-Apt sensor interface can reduce the hopping rate of charge carriers (holes) in the CPMCNFs, which is probably responsible for the decrease in current.[42] The negative charge of the CPB-Apt sensor reduced to limit of detect level that is generally considered a significant signal when the signal-to-noise ratio is greater than or equal to 3.0 with decreasing

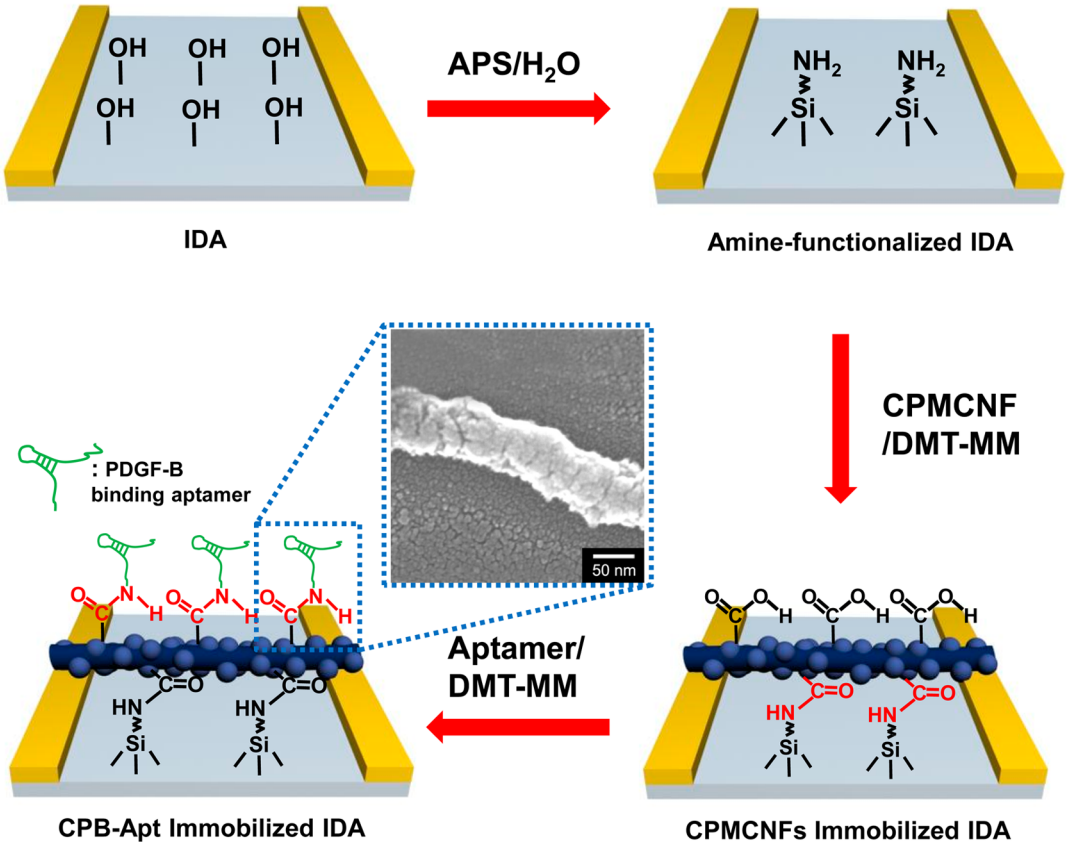

Figure 4. Synthetic protocol of immobilization of CPMCNF-aptamer tranducers on the interdigitated array electrode substrate.

concentration of target analyte.[40] The limit of detection of the CPB-Apt sensor was 5 fM (signal-to-noise ratio: 3.4) for PDGF-BB, lower than those of other aptamer-based PDGF sensor and carboxylated polypyrrole coated pristine CNF without metaloxide nanonodule (see Supporting Information, Figure S2).[43,44] Additionally, PDGF-AB detected as low as 500 fM and injection of PDGF-AA did not induce current changes because the PDGF-A chain had no affinity for the PDGF-B binding aptamer.

Figure 6b shows the calibration curve of the sensitivity of the CPB-Apt FET sensor. The sensitivity (S) was determined from the normalized current change $((\Delta I/I_0)_{sp} \times 100)$ saturation point, measured after a 10s of the analyte addition was inserted. The sensitivity was enhanced with increasing concentrations from 5×10^0 to 5×10^4 fM of the PDGF-BB and from 5×10^2 to 5×10^4 fM of PDGF-AB, respectively. Importantly, the sensitivity of CPB-Apt sensor to PDGF-BB was higher than that of PDGF-AB over a wide range of concentrations. Also, there was no current change with increasing injection amounts of PDGF-AA in the FET sensor device due to the absence of any affinity with the PDGF-B binding aptamer.

To test the selectivity of the CPB-Apt FET sensor for PDGF-B analysis, control experiments were conducted using other biological components. Figure 7a shows the selectivity of the CPB-Apt FET sensor toward the three variants of PDGF and other biomolecules, including bovine serum albumin (BSA), ATP, and calmodulin (Cal). During the real-time selectivity test, insignificant changes in I_{sd} were observed on the addition of nontarget molecules such as BSA, ATP, Cal, and PDGF-AA. Furthermore, there was a difference in I_{sd} with the two types of PDGF (PDGF-AB, and PDGF-BB) because the PDGF-B binding aptamer had no affinity for the PDGF-A chain. In addition, CPB-Apt sensor displayed significant I_{sd} changes at 5 fM of PDGF-BB, however, did not show any significant signals of PDGF-AB (Figure 7b). Thus, the CPB-Apt FET sensor showed higher specificity for PDGF-BB, which is composed only of PDGF-B chains, than for PDGF-AB, which is composed of both A and B chains. These results demonstrated the high selectivity of the CPB-Apt FET sensor.

Figure 8 suggests the reusability of the CPB-Apt FET sensor system based on sensitivity changes to a constant concentration (50 pM) of the three variant PDGFs. To demonstrate the reusability of the CPB-Apt sensor, a three-step process was conducted. First, the used CPB-Apt sensor was washed with sodium chloride solution, which causes disruption of the hydrogen bonding and electrostatic interactions responsible for most of the aptamer−target association. Second, it was rinsed with distilled water and air-dried for removing salt residue.[45,46] Then, injections of target biomolecules were carried out several times at an injection interval of 3 days. The sensitivity of the CPB-Apt sensor system to the three variants of PDGF was generally consistent during the repeated tests, although the sensitivity decreased slightly due to aptamer degradation. The covalent anchoring of the electrode substrate/CPMCNFs and CPMCNF/binding aptamers provided stability for long-term reusability. On the basis of these data, this covalent anchoring aptamer sensor can be successfully reused in consecutive assays.

CONCLUSION

In summary, we successfully fabricated a FET system sensor transistor using PDGF-B binding aptamer-conjugated CPMCNFs as a transducer. The CPMCNFs was fabricated

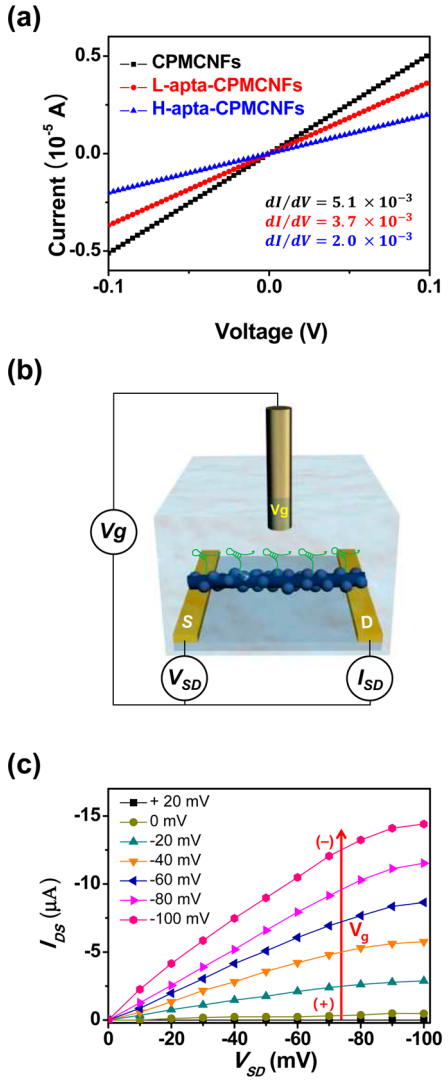

Figure 5. (a) Current−voltage (I−V) curves of aptamer-conjugated CPMCNF immobilized IDA electrode (black, without aptamer; red, low concentration of conjugated-aptamer; blue, high concentration of conjugated-aptamer). (b) Schematic diagram of a liquid-ion gated FET sensor using aptamer-conjugated CPMCNFs. (c) I_{sd}−V_{sd} output characteristic of CPMCNFs-aptamer liquid-ion gated FET sensor different gate voltage (V_g) from +20 to −100 mV in step of −20 mV (scan rate of V_{sd}: 10 mV s^{-1}).

via single-nozzle coelectrospinning and vapor deposition polymerization (VDP). Due to the zinc oxide nanonodules on the MCNF surface, there was no need for any further treatment for surface functionalization to form the CPPy layer. Then, the CPMCNFs were immobilized on the IDA substrate and bonded to the amine-modified PDGF-B binding aptamer by amide covalent bonding. The CPMCNFs-aptamer (CPB-Abt) FET sensor system showed real-time responses and a very low detection level (5 fM) for PDGF-BB. Additionally, the CPB-Apt sensor displayed high selectivity for PDGF-BB. Furthermore, the CPB-Apt sensor was reusable over a long period because of the covalent bonding of each component. From a sensor performance point of view, the CPB-Apt FET sensor should be applicable over a wide range of applications in biological and environmental research.

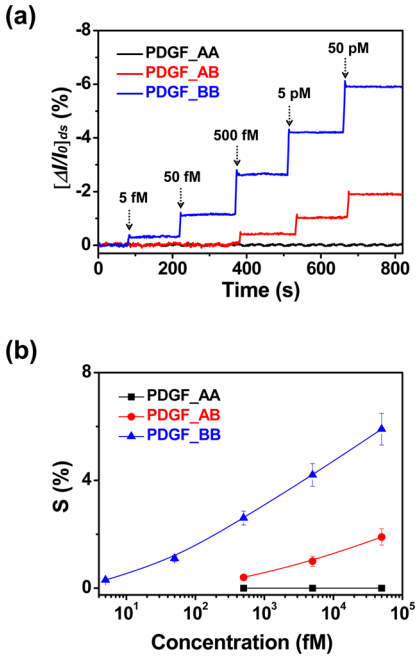

Figure 6. (a) Real-time responses with normalized current changes (V_g, 50 mV; V_{sd}, 50 mV) and (b) calibration curve of CPB-Apt FET sensor toward three variants of PDGF with different concentration (black, PDGF_AA; red, PDGF_AB; blue, PDGF_BB).

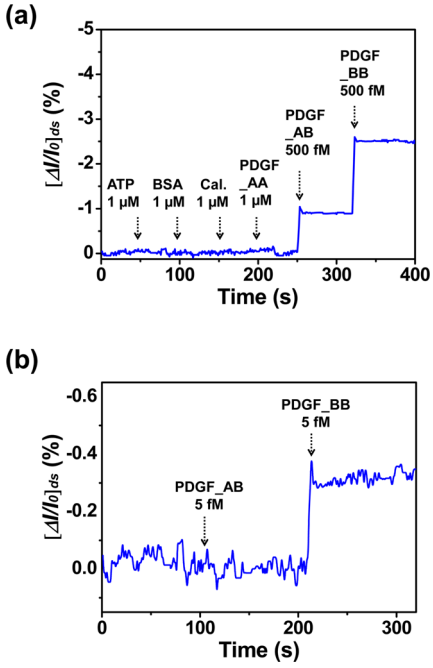

Figure 7. Real-time selective responses of CPB-Apt FET sensor toward (a) 1 μM of nontarget molecules (ATP, BSA, Calmoduline (Cal), PDGF-AA) and 500 fM of target molecules (PDGF-BB and PDGF-AB) and (b) 5 fM of different target molecules (V_g, 50 mV; V_{sd}, 50 mV).

MATERIALS AND METHODS

Materials. Poly(acrylonitrile) (PAN, Mw = 150 000), poly-(vinylpyrrolidone) (PVP, Mw = 1 300 000), zinc acetate (ZnAc2), pyrrole, and pyrrole-3-carboxylic acid were purchased from Sigma. The platelet-derived growth factor-B (PDGF-B) binding aptamer was from Bioneer Co. (Dajeon, Korea). The PDGF-B binding aptamer was modified at the 5′ terminus with an amine group, and its sequence was

dx.doi.org/10.1021/am5032693 | ACS Appl. Mater. Interfaces 2014, 6, 13859−13865

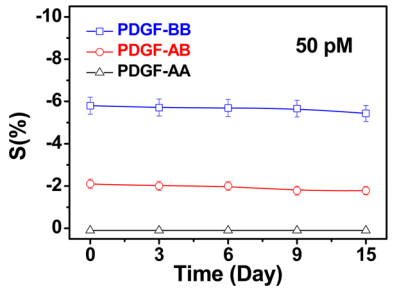

Figure 8. Reusability test of the CPB-Apt FET sensor system toward three variants of PDGF at 50 pM concentration (black, PDGF-AA; red, PDGF-AB; blue, PDGF-BB).

as follows: 5′ NH_2 CAG GCT ACG GCA CGT AGA GCA TCA CCA TGA TCC TG 3′. PDGF-BB, PDGF-AB, PDGF-AA, adenosine, triphosphate (ATP), and calmodulin (Cal) were purchased from Aldrich as analyte materials.

Fabrication of MCNFs. Metal oxide-decorated CNFs (MCNFs) were fabricated as starting materials. PAN solutions were prepared by dissolving 1.0 gof PAN in 10 mL of DMF at 80−90 °C for 1 h with vigorous stirring. PVP solutions were prepared by dissolving 1 g of PVP and 0.3 g of $ZnAc_2$ in 10 mL of DMF at 50 °C for 2 h with vigorous stirring. Then, the PAN and PVP solutions were mixed at 80−90 °C for 3 h. The resulting viscous hybrid solution was injected from a syringe (10 mL) using a single-nozzle coelectrospinning method. The syringe for electrospinning was filled with hybrid solution. The electrospinning needle diameter was 30 guage (OD, 0.40 mm; ID, 0.20 mm). The needle was connected to the positive terminal of a power supply. The voltage was conducted at 17 kV, and the solution was delivered to the syringe by the syringe pump. The flow rate of the syringe pump was fixed at 10 μL/min. The distance of tip to collector was fixed at 15 cm. The electrospun NFs were heated at 400 °C for 2 h to calcine and then heated in flowing argon gas at 800 °C for 1 h for carbonization.

Fabrication of CPMCNFs. Carboxylated polypyrrole-coated hybrid carbon nanofibers (CPMCNFs) were prepared by vapor deposition polymerization (VDP) of the MCNFs. First, 0.5 g of MCNFs was soaked in 10 mL of ethanolic ferric chloride ($FeCl_3$) solution (0.1M) for 5 min. Then, the soaked MCNFs were dried in a vacuum oven for 4 h and inserted inside the reactor with 0.18 mmol pyrrole-3-carboxylic acid. The internal pressure was then reduced to 10^{-2} Torr, and the reactor was moved into the 60 °C oven for 10 min. After the VDP process, approximately 0.5 g of CPMCNFs was gained with little loss.

Fabrication of the CPB-Apt FET Sensor. To construct the CPMCNFs-aptamer FET sensor, the IDA substrate was first treated with 5 wt % aqueous amino silane (3-aminopropyltrime-thoxysilane, APS) for 6 h to introduce amino groups on the IDA substrate. It was then exposed to a mixture of 0.1 wt % aqueous CPMCNFs solution (40 μL) and 1 wt % aqueous 4-(4,6-dimethoxy-1,3,5-triazin-2-yl)-4-methylmorpholinium chloride (DMT-MM, 40 μL) solution for 12 h. The resulting CPMCNFs-immobilized substrate was rinsed with distilled water. Subsequently, the coupling reaction to attach the PDGF-B binding aptamer to the CPMCNF surface was carried out using a mixture of PDGF-B binding aptamer and 1 wt % aqueous DMT-MM (40 μL) for 12 h. Then, the platform substrate was rinsed with distilled water and dried at room temperature.

Characterization. TEM and HRTEM images were obtained with JEOL JEM-200CX and JEOL JEM-3010 microscopes, respectively. A JEOL 6700 instrument was used to obtain field emission scanning electron microscopy (FE-SEM) images. IR data were obtained with a Bomem MB 100 (Quebec, Canada) in absorption mode.

Electrical Measurements with the CPB-Apt Sensor. All electrical measurements were conducted with a Keithley 2612A source meter and probe station (MS TECH, model 4000) and a Wonatech WBCS 3000 potentiostat. A chamber (300 μL volume) was designed and used for solution-based measurements. The current change was normalized as

$$\left[\frac{\Delta I}{I_0}\right]_{SD}(\%) = \frac{(I - I_0)}{I_0} \times 100 \quad (1)$$

where I_0 is the initial current, and I is the measured real-time current.

■ ASSOCIATED CONTENT

Supporting Information

(1) SEM and TEM images of metal oxide decorated carbon nanofiber; (2) control experiment using CPMCNFs without binding aptamer and carboxylated polypyrrole decorated CNFs-aptamer. This material is available free of charge via the Internet at http://pubs.acs.org.

■ AUTHOR INFORMATION

Corresponding Author

*J. Jang. Tel: 82-2-880-8348. Fax: +82-2-888-7295. E-mail: jsjang@plaza.snu.ac.kr.

Notes

The authors declare no competing financial interest.

■ ACKNOWLEDGMENTS

This research was supported by the National Research Foundation of Korea (NRF) grant funded by the Korea government(MEST) (No. 2011-0017125).

■ REFERENCES

(1) Han, J.; Sudheendra, L.; Kim, H.; Gee, S. J.; Hammock, B. D.; Kennedy, I. M. Ultrasensitive On-Chip Immuno Assays with a Nanoparticle-Assembled Photonic Crystal. *ACS Nano* **2012**, *6*, 8570−8582.

(2) Li, M.; Cushing, S. K.; Zhang, J.; Suri, S.; Evans, R.; Petros, W. P.; Gibson, L. F.; Ma, D.; Liu, Y.; Wu, N. Three-Dimensional Hierarchical Plasmonic Nano-Architecture Enhanced Surface-Enhanced Raman Scattering Immunosensor for Cancer Biomarker Detection in Blood Plasma. *ACS Nano* **2013**, *7*, 4967−4976.

(3) Kwon, O. S.; Park, S. J.; Hong, J.; Han, A.; Lee, J. S.; Lee, J. S.; Oh, J. H.; Jang, J. Flexible FET-Type VEGF Aptasensor Based on Nitrogen-Doped Graphene Converted from Conducting Polymer. *ACS Nano* **2012**, *6*, 1486−1493.

(4) He, X.-P.; Deng, Q.; Cai, L.; Wang, C.-Z.; Zang, Y.; Jia, Li; Chen, G.-R.; Tian, H. Fluorogenic Resveratrol-Confined Graphene Oxide for Economic and Rapid Detection of Alzheimer's Disease. *ACS Appl. Mater. Interfaces* **2014**, *6*, 5379−5382.

(5) Yu, X.; Munge, B.; Patel, V.; Jensen, G.; Bhirde, A.; Gong, J. D.; Kim, S. N.; Gillespie, J.; Gutkind, J. S.; Papadimitrakopoulos, F.; Rusling, J. F. Carbon Nanotube Amplification Strategies for Highly Sensitive Immunodetection of Cancer Biomarkers. *J. Am. Chem. Soc.* **2006**, *128*, 11199−11205.

(6) Shukoor, M. I.; Altman, M. O.; Han, D.; Bayrac, A. T.; Ocsoy, I.; Zhu, Z.; Tan, W. Aptamer-Nanoparticle Assembly for Logic-Based Detection. *ACS Appl. Mater. Interfaces* **2012**, *4*, 3007−3011.

(7) Yoon, H.; Jang, J. Conducting-Polymer Nanomaterials for High-Performance Sensor Applications: Issues and Challenges. *Adv. Funct. Mater.* **2009**, *19*, 1567−1576.

(8) Heister, E.; Brunner, E. W.; Dieckmann, G. R.; Jurewicz, I.; Dalton, A. B. Are Carbon Nanotubes a Natural Solution? Applications in Biology and Medicine. *ACS Appl. Mater. Interfaces* **2013**, *5*, 1870−1891.

(9) Kim, D.-J.; Park, H.-C.; Sohn, I. Y.; Jung, J.-H.; Yoon, O. J.; Park, J.-S.; Yoon, M.-Y.; Lee, N.-E. Electrical Graphene Aptasensor for Ultra-Sensitive Detection of Anthrax Toxin with Amplified Signal Transduction. *Small* **2013**, *19*, 3352−3360.

(10) Sumedha, J. D. Aptamers: An Emerging Class of Molecules That Rival Antibodies in Diagnostics. *Clin. Chem.* **1999**, *25*, 1628−1650.
(11) Barst, R. J. PDGF Signaling in Pulmonary Arterial Hypertension. *J. Clin. Invest.* **2005**, *115*, 2691−2694.
(12) Lassila, M.; Allen, T. J.; Cao, Z.; Thallas, V.; J-Dahm, K. A.; Candido, R.; Cooper, M. E. Imatinib Attenuates Diabetes-Associated Atherosclerosis. *Arterioscler., Thromb., Vasc. Biol.* **2004**, *24*, 935−942.
(13) Szabó, A.; Laki, J.; Madsen, H. O.; Dósa, E.; Prohászka, Z.; Rugonfalvi-Kiss, S.; Kókai, M.; Acsádi, G.; Karádi, I.; Entz, L.; Selmeci, L.; Romics, L.; Füst, G.; Garred, P. Early Rise in Serum VEGF and PDGF Levels Predisposes Patients with a Normal MBL2 Genotype to Restenosis After Eversion Endarterectomy. *Stroke* **2007**, *38*, 2247−2253.
(14) Trojanowska, M. Role of PDGF in Fibrotic Diseases and Systemic Sclerosis. *Rheumatology* **2008**, *47*, v2−v4.
(15) Shih, A. H.; Dai, C.; Hu, X.; Rosenblum, M. K.; Koutcher, J. A.; Holland, E. C. Dose-Dependent Effects of Platelet-Derived Growth Factor-B on Glial Tumorigenesis. *Cancer Res.* **2004**, *64*, 4783−4789.
(16) Penmatsa, V.; Ruslinda, A. R.; Beidaghi, M.; Kawarada, H.; Wang, C. Platelet Derived Growth Factor Oncoprotein Detection Using Three-Dimensional Carbon Microarrays. *Biosens. Bioelectron.* **2013**, *39*, 118−123.
(17) Vicens, M. C.; Sen, A.; Vanderlaan, A.; Drake, T. J.; Tan, W. Investigation of Molecular Beacon Aptamer-Based Bioassay for Platelet-Derived Growth Factor Detection. *ChemBioChem* **2005**, *6*, 900−907.
(18) Yang, C. J.; Jockusch, S.; Vicens, M.; Turro, N. J.; Tan, W. Light-Switching Excimer Probes for Rapid Protein Monitoring in Complex Biological Fluids. *Proc. Natl. Acad. Sci. U. S. A.* **2005**, *102*, 17278−17283.
(19) Plante, M.-P.; Berube, E.; Bissonnette, L.; Bergeron, M. G.; Leclerc, M. Polythiophene Biosensor for Rapid Detection of Microbial Particles in Water. *ACS Appl. Mater. Interfaces* **2013**, *5*, 4544−4548.
(20) Wang, Y.; Zhou, F.; Liu, X.; Yuan, L.; Li, D.; Wang, Y.; Chen, H. Aptamer-Modified Micro/Nanostructured Surfaces: Efficient Capture of Ramos Cells in Serum Environment. *ACS Appl. Mater. Interfaces* **2013**, *5*, 3816−3823.
(21) Ruslinda, A. R.; Penmatsa, V.; Ishii, Y.; Tajima, S.; Kawarada, H. Highly Sensitive Detection of Platelet-Derived Growth Factor on a Functionalized Diamond Surface Using Aptamer Sandwich Design. *Analyst* **2012**, *137*, 1692−1697.
(22) Fang, X.; Sen, A.; Vicens, M.; Tan, W. Synthetic DNA Aptamers to Detect Protein Molecular Variants in a High-Throughput Fluorescence Quenching Assay. *ChemBioChem* **2003**, *4*, 829−834.
(23) Lai, R. Y.; Plaxco, K. W.; Heeger, A. J. Aptamer-based Electrochemical Detection of Picomolar Platelet-Derived Growth Factor Directly in Blood Serum. *Anal. Chem.* **2007**, *79*, 229−233.
(24) Degefa, T. H.; Kwak, J. Label-Free Aptasensor for Platelet-Derived Growth Factor (PDGF) Protein. *Anal. Chim. Acta* **2008**, *613*, 163−168.
(25) Robertson, J. Realistic Application of CNTs. *Mater. Today* **2004**, *7*, 46−52.
(26) Trojanowicz, M. Analytical Applications of Carbon Nanotubes: A Review. *Trends Anal. Chem.* **2006**, *25*, 480−489.
(27) Qi, P.; Vermesh, O.; Javey, M. A.; Wang, Q.; Dai, H.; Peng, S.; Cho, K. J. Toward Large Arrays of Multiplex Functionalized Carbon Nanotube Sensors for Highly Sensitive and Selective Molecular Detection. *Nano Lett.* **2003**, *3*, 347−351.
(28) So, H.-M; Park, D.-W.; Jeon, E.-K.; Kim, Y.-H.; Kim, B. S.; Lee, C.-K.; Choi, S. Y.; Kim, S. C.; Chang, H.; Lee, J.-O. Detection and Titer Estimation of Escherichiacoli Using Aptamer-Functionalized Single-Walled Carbon-Nanotube Field-Effect Transistors. *Small* **2008**, *2*, 197−201.
(29) Rand, E.; Periyakaruppan, A.; Tanaka, Z.; Zhang, D. A.; Marsh, M. P.; Andrews, R. J.; Lee, K. H.; Chen, B.; Meyyappan, M.; Koehne, J. E. A Carbon Nanofiber Based Biosensor for Simultaneous Detection of Dopamine and Serotonin in The Presence of Ascorbic Acid. *Biosens. Bioelectron.* **2013**, *42*, 434−438.
(30) Koehne, J. E.; Chen, H.; Cassell, A.; Liu, G-y.; Li, J.; Meyyappan, M. Arrays of Carbon Nanofibers as a Platform for Biosensing at the Molecular Level and for Tissue Engineering and Implantation. *Bio-Med. Mater. Eng.* **2009**, *19*, 35−43.
(31) Wua, L.; Zhangb, X.; Jua, H. Amperometric Glucose Sensor Based on Catalytic Reduction of Dissolved Oxygen at Soluble Carbon Nanofiber. *Biosens. Bioelectron.* **2007**, *23*, 479−484.
(32) Lee, J. S.; Kown, O. S.; Park, S. J.; Park, E. Y.; You, S. A.; Yoon, H.; Jang, J. Fabrication of Ultrafine Metal-Oxide-Decorated Carbon Nanofibers for DMMP Sensor Application. *ACS Nano* **2011**, *5*, 7992−8001.
(33) Lee, J. S.; Kown, O. S.; Shin, D. H. J.; Jang. WO3 Nanonodule-Decorated Hybrid Carbon Nanofibers for NO_2 Gas Sensor Application. *J. Mater. Chem. A* **2013**, *1*, 9099−9106.
(34) Zhang, H.; Zhong, X.; Xu, J.-J.; Chen, H.-Y. Fe_3O_4/Polypyrrole/Au Nanocomposites with Core/Shell/Shell Structure: Synthesis, Characterization, and Their Electrochemical Properties. *Langmuir* **2008**, *24*, 13748−13752.
(35) Shin, D. H.; Lee, J. S.; Jun, J. Fabrication of Amorphous Carbon-Coated NiO Nanofibers for Electrochemical Capacitor Applications. *J. Mater. Chem. A* **2014**, *2*, 3364−3371.
(36) Jang, J.; Bae, J. Carbon Nanofiber/Polypyrrole Nanocable as Toxic Gas Sensor. *Sens. Actuators, B* **2007**, *122*, 7−13.
(37) Vetter, C. A.; Suryawanshi, A.; Lamb, J. R.; Law, B.; Gelling, V. J. Novel Synthesis of Stable Polypyrrole Nanospheres Using Ozone. *Langmuir* **2011**, *27*, 13719−13728.
(38) Fujii, S.; Matsuzawa, S.; Hamasaki, H.; Nakamura, Y. Polypyrrole−Palladium Nanocomposite Coating of Micrometer-Sized Polymer Particles Toward a Recyclable Catalyst. *Langmuir* **2012**, *28*, 2436−2447.
(39) Yoon, H.; Lee, S. H.; Kwon, O. S.; Song, H. S.; Oh, E. H.; Park, T. H.; Jang, J. Polypyrrole Nanotubes Conjugated with Human Olfactory Receptors: High-Performance Transducers for FET-Type Bioelectronic Noses. *Angew. Chem., Int. Ed.* **2009**, *48*, 2755−2758.
(40) Kwon, O. S.; Park, S. J.; Jang, J. A High-Performance VEGF Aptamer Functionalized Polypyrrole Nanotube Biosensor. *Biomaterials* **2010**, *31*, 4740−4747.
(41) Huang, X.-J.; O'Mahony, A. M.; Compton, R. G. Microelectrode Arrays for Electrochemistry: Approaches to Fabrication. *Small* **2009**, *7*, 776−788.
(42) Xie, H.; Luo, S.-C.; Yu, H. Electric-Field-Assisted Growth of Functionalized Poly(3,4-ethylenedioxythiophene) Nanowires for Label-Free Protein Detection. *Small* **2009**, *22*, 2611−2617.
(43) Wu, Z.-S.; Zhou, H.; Zhang, S.; Shen, G.; Yu, R. Electrochemical Aptameric Recognition System for a Sensitive Protein Assay Based on Specific Target Binding-Induced Rolling Circle Amplification. *Anal. Chem.* **2010**, *82*, 2282−2289.
(44) Hu, H.; Li, H.; Zhao, Y.; Dong, S.; Li, W.; Qiang, W.; Xu, D. Aptamer-Functionalized Silver Nanoparticles for Scanometricdetection of Platelet-Derived Growth Factor-BB. *Anal. Chim. Acta* **2014**, *812*, 152−160.
(45) Guo, L.; Kim, D.-H. LSPR Biomolecular Assay with High Sensitivity Induced by Aptamer−Antigen−Antibody Sandwich Complex. *Biosens. Bioelectron.* **2012**, *31*, 567−570.
(46) Park, J.-H.; Byun, J.-Y.; Mun, H.; Shim, W.-B.; Li, T.; Kim, M.-G. A Regeneratable, Label-Free, Localized Surface Plasmon Resonance (LSPR) Aptasensor for The Detection of Ochratoxin A. *Biosens. Bioelectron.* **2014**, *59*, 321−327.